Eur Radiol (2015) 25:2362–2370
DOI 10.1007/s00330-015-3656-9

COMPUTED TOMOGRAPHY

Use of Model-Based Iterative Reconstruction (MBIR) in reduced-dose CT for routine follow-up of patients with malignant lymphoma: dose savings, image quality and phantom study

Edouard Hérin · François Gardavaud · Mélanie Chiaradia · Pauline Beaussart · Philippe Richard · Madeleine Cavet · Jean-François Deux · Corinne Haioun · Emmanuel Itti · Alain Rahmouni · Alain Luciani

Received: 9 December 2014 / Accepted: 3 February 2015 / Published online: 8 March 2015

Abstract
Objectives To evaluate both in vivo and in phantom studies, dose reduction, and image quality of body CT reconstructed with model-based iterative reconstruction (MBIR), performed during patient follow-ups for lymphoma.
Methods This study included 40 patients (mean age 49 years) with lymphoma. All underwent reduced-dose CT during follow-up, reconstructed using MBIR or 50 % advanced statistical iterative reconstruction (ASIR). All had previously undergone a standard dose CT with filtered back projection (FBP) reconstruction. The volume CT dose index (CTDIvol), the density measures in liver, spleen, fat, air, and muscle, and the image quality (noise and signal to noise ratio, SNR) (ANOVA) observed using standard or reduced-dose CT were compared both in patients and a phantom study (Catphan 600) (Kruskal Wallis).
Results The CTDIvol was decreased on reduced-dose body CT (4.06 mGy vs. 15.64 mGy $p<0.0001$). SNR was higher in reduced-dose CT reconstructed with MBIR than in 50 % ASIR or than standard dose CT with FBP (patients, $p\leq0.01$; phantoms, $p=0.003$). Low contrast detectability and spatial resolution in phantoms were not altered on MBIR-reconstructed CT ($p\geq0.11$).
Conclusion Reduced-dose CT with MBIR reconstruction can decrease radiation dose delivered to patients with lymphoma, while keeping an image quality similar to that obtained on standard-dose CT.
Key Points
- *In lymphoma patients, CT dose reduction is a major concern.*
- *Reduced-dose body CT provides a fourfold radiation dose reduction.*
- *Optimized CT reconstruction techniques (MBIR) can maintain image quality.*

Keywords Computed tomography · Radiation dosage · Image processing, computer-assisted · Lymphoma · Image enhancement

E. Hérin · F. Gardavaud · M. Chiaradia · P. Beaussart · M. Cavet · J.-F. Deux · A. Rahmouni · A. Luciani
AP-HP, Hôpitaux Universitaires Henri Mondor, Imagerie Médicale, Créteil 94010, France

E. Hérin · M. Chiaradia · M. Cavet · J.-F. Deux · C. Haioun · E. Itti · A. Rahmouni · A. Luciani
Faculté de Médecine, Université Paris Est Créteil, Créteil 94010, France

P. Richard
GE Healthcare France, Buc, France

C. Haioun
AP-HP, Hôpitaux Universitaires Henri Mondor, Hémopathies Lymphoïdes, Créteil 94010, France

E. Itti
AP-HP, Hôpitaux Universitaires Henri Mondor, Médecine Nucléaire, Créteil 94010, France

A. Luciani
INSERM Unité U 955, Equipe 18, Créteil 94010, France

A. Luciani (✉)
AP-HP, Groupe Henri Mondor Albert Chenevier, Imagerie Médicale, CHU Henri Mondor, 51 Avenue du Maréchal de Lattre de Tassigny, 94010 Créteil Cedex, France
e-mail: alain.luciani@hmn.aphp.fr

Introduction

During the past several years, medical radiation exposure has increased mostly because of the growing use of computed tomography (CT) [1–3]. Recent studies have stressed the potential relationship between medical radiation exposure and the risk of developing cancer [4–8]. Patients undergoing repeated CTs seem the most at risk of developing radiation-induced diseases, although this result is still debated [9–11]. Patients with lymphoma often have a high survival rate; 80 % to 90 % of them are alive 3 years after treatment [12]. These patients may be young at the time of the diagnosis and may have an extended survival without relapse leading to repeated follow-up CT [13–15]. As effects of medical radiation on outcome are still unclear, it is wise to apply the ALARA principle, especially in this specific population [16].

Despite the key role of PET-CT in aggressive lymphoma patient management, CT for lymphoma follow-up is indicated in patients with indolent lymphomas, diffuse large B-cell lymphoma (DLBCL) with international prognosis index (IPI) ≥3 and patients included in clinical trials, as recently confirmed in expert recommendations [17]. CT also plays a significant role in various other lymphoma histologies both at diagnosis and follow-up according to the latest European Society for Medical Oncology (ESMO) or National Comprehensive Cancer Network (NCCN) guidelines [13–15].

CT dose reduction strategies rely on decreasing radiation output of the CT tube, inducing a higher level of image noise. Traditionally, images have been reconstructed from CT data using analytical reconstruction algorithms such as filtered back-projection (FBP). But noise and artefact reductions are necessary steps towards a further dose reduction in CT [18, 19]. Hence, all CT manufacturers have developed new reconstruction algorithms [20] including iterative reconstruction techniques such as adaptive statistical iterative reconstruction (ASIR) [21–25]. More recently, a complex model-based iterative reconstruction method (MBIR, Veo®, GE Healthcare, WI, USA) has been reported [26, 27]. MBIR allows the modelling of projection and electronic noise, and introduces optic chain modelling for greater noise reduction. The use of MBIR has been reported in various fields including paediatric imaging [28], chest examinations [29] and oncology patients [30].

The objective of our study was to evaluate both in vivo and in phantom studies, the dose reduction and image quality of reduced-dose body CT, reconstructed with MBIR, performed during the follow-up of lymphoma patients.

Materials and methods

The study was approved by our institutional review board and the requirement for informed consent was waived. The industry-independent authors maintained full control of the data at all times.

Study population

Between September 2012 and December 2013, 45 consecutive patients referred to our institution for the CT follow-up of Hodgkin or non-Hodgkin lymphoma in complete remission according to 2007 Cheson's criteria [31] (n=41), or with stable indolent lymphoma (n=4) were considered eligible for this retrospective study. Five patients for whom no prior CT performed at our institution less than 48 months before referral was available were excluded. As a result, 40 patients were finally included (see Table 1 for population description). On referral, the median overall follow-up time of all patients was 32 months (mean=35 months, range 9 to 96 months). Following reduced-dose CT, 35 patients were considered in persistent complete response, four patients with indolent lymphoma were considered stable and remained untreated, and one patient was considered as showing disease relapse (confirmed with biopsy). Following the reduced-dose CT, the median follow-up was 15.7 months (range 7 to 23 months).

Table 1 Study population

Specifications	Our population
Age (years)	Mean: 49; range, 20 – 80
Male/Female	30/10
Ann Arbor initial staging	6 stage I, 11 stage II 5 stage III 18 stage IV
Type of lymphomas	16 Hodgkin Lymphoma 10 Diffuse Large B-Cell Lymphoma 4 Follicular Lymphoma 2 Mantle B-Cell Lymphoma 2 Peripheral T-Cell Lymphoma 6 Others
Delay between complete remission and date of reduced-dose CT scan	Mean (months): 25.7 Range (months): 2-102
Response status according to 2007 Cheson's criteria [31] using the reduced-dose CT scan	35 maintained complete response 1 Disease Relapse (confirmed with PET-CT and biopsy) 4 Patients with stable disease with no treatment (indolent lymphoma, only active surveillance)
Follow up duration after reduced-dose CT scan	Mean (months): 15.7 Range (months): 7-23

CT technique

Reduced-dose CT All included patients underwent reduced-dose body CT - including neck, chest, abdomen, and pelvis coverage - at our institution on a 64-row MDCT system (HD 750 Discovery, GE Healthcare, Milwaukee, WI, USA). Scan parameters are described in Table 2. All images were reconstructed using raw-data acquisitions. Both native, 50 % ASIR, and MBIR images were reconstructed. A 50 % ASIR level was selected as it appears to be a good compromise for reducing noise without affecting image quality [19].

Standard dose CT All included patients had previously undergone, at our institution, a standard-dose follow-up CT on a 64-slice MDCT (Lightspeed VCT®, GE Healthcare, Milwaukee, WI, USA), called standard-dose CT, at a mean delay of 20 months prior to the reduced dose CT. Imaging parameters are also shown in Table 2. All standard-dose CTs were full filtered back projections reconstructed without iterative reconstructions. All standard-dose CT examinations complied with national reference dose recommendations.

For both standard-dose CT scan and reduced-dose CT scan, a monophasic contrast enhanced CT (CECT) acquisition was performed covering the cervical region to the pelvic groin, initiated at portal phase 70 s after the injection of 1.5 cc/kg of iomeprol 350 (Iomeron 350, Bracco Imaging France, Courcouronnes, France) at a 3.5 cc/sec injection rate.

Reconstruction of standard-dose and reduced-dose CT For all CTs, post-processing reconstructions were performed on all native data in the transverse plane to yield 2.5-mm-thick sections, allowing comparison between reconstruction techniques.

Table 2 CT image acquisition parameters of reduced-dose CT and of standard-dose CT

CT imaging parameters	Reduced-dose CT (ASIR- and MBIR-reconstructed)	Standard-dose CT (FBP-reconstructed)
Slice thickness (mm)	0.625	1.25
Kilovoltage (kV)	100	120
Rotation time (s)	0.7	0.6
mA modulation (range)	100-300	150-650
mA observed on 40 patients acquisitions (mean)	130	365
Pitch	1.375	1.375
Noise index (HU)	60	25
Advanced Statistical Iterative Reconstruction (ASIR®) (%)	50	N/A
Model-Based Iterative Reconstruction (MBIR)	Yes	No
Kernel	Standard	Standard
Field of View (FOV)	Large body	Large body

Dosimetric analysis

For each reduced-dose and standard-dose CT scan, the following parameters were collected including CTDIvol (volume computed tomography dose index), length of helical acquisition, and dose length product (DLP).

Image analysis

For all reconstructed images – namely FBP reconstructed standard-dose CT images, and both 50 % ASIR and MBIR reconstructed images on reduced-dose CT – the mean density (HU), the noise – defined as the standard deviation (SD) of each density measurements – and the signal-to-noise ratio (SNR) of the liver, spleen, abdominal subcutaneous fat, lumbar muscle, and air were determined. The SNR for each organ was defined as follows (Eq. 1):

$$SNR = \frac{D}{SD}$$

Where D is the mean density for each organ and SD the mean standard deviation of density within the regions of interest (ROIs) described below.

Three identically sized ROIs (mean size = 100 mm^2 +/- 10 %) were manually positioned on the liver, carefully avoiding liver vessels or heterogeneous liver segments. In a similar manner, two ROIs, of the same dimension, were positioned within the spleen parenchyma, two ROIs within the lumbar muscle, two ROIs within the abdominal sub cutaneous fat, and two ROIs within the anterior-located air. All ROIs were placed by two of the authors (E.H. and A.L., with a respective 3 and 15 years experience in CT) on all reconstructed acquisitions – FBP of standard-dose CT, 50 % ASIR, and MBIR reconstructed images for reduced-dose CT – and were automatically synchronized, using integrated registration software (GE Healthcare), allowing the propagation of each ROI when scrolling different acquisitions at the same anatomical location.

Phantom study

A CATPHAN 600 phantom (The Phantom Laboratory, Greenwich, NY, USA) was included in this study for quality control. This cylindrical phantom allows the determination of low contrast detectability, signal to noise ratio, and spatial resolution in z and x-y planes. The phantom was imaged on both CT devices (Lightspeed VCT and Discovery 750) using the same parameters used in the clinical study besides the tube current, which was set at a constant 365 mA, and 130 mA for the standard-dose CT (Lightspeed VCT) and reduced-dose CT (Discovery 750), respectively. Chosen mA corresponds to the

Table 3 Dosimetric comparison of standard-dose CT and of reduced-dose CT acquisitions

Dosimetric parameters	Reduced-dose CT (ASIR- and MBIR-reconstructed)	Standard-dose CT (FBP-reconstructed)	*p* (Two independent samples t-test)
CTDIvol (mGy) [mean±SD]	4.06±1.1	15.6±4.2	$p<0.0001$
DLP (mGy.cm) [mean±SD]	345±99	1,252±339	$p<0.0001$
Length of acquisition (cm) [mean±SD]	78.8±6.3	75.0±7.6	$p=0.018$

mean mA values observed in the study population on each machine whether with the standard-dose or the reduced-dose CT imaging parameters.

Native raw data obtained were 1.25 mm thickness with FBP or ASIR, and 0.625 mm with MBIR reconstruction technique. For MBIR acquisition, post-processing reconstructions was performed on native data, in the transverse plane to yield 1.25-mm-thick sections, allowing comparison between reconstruction techniques.

Quantitative and qualitative phantom analysis All qualitative phantom analyses were performed independently by two readers (E.H. and A.L. with a respective 3 and 15 years experience in CT), blinded to the type of acquisition and reconstruction assessed. The low contrast detectability and the highest spatial resolution were qualitatively evaluated. The signal to noise ratio was quantified by a single reader (F.G.), for each acquisition and reconstruction. Five phantom acquisitions using the standard-dose and the reduced-dose CT scan parameters were evaluated by each reader.

– *Low contrast detectability:*

To evaluate low contrast detectability, the Catphan 600 phantom contains a total of nine targets varying in both maximum transverse diameter (namely 2 mm to 15 mm) and contrast level (namely 1 %, 0.5 %, and 0.3 %). The two readers independently determined how many targets they could entirely see for each acquisition and reconstruction.

– *Spatial resolution:*

To allow spatial resolution quantification in the transverse plane, the Catphan phantom contains spaced aluminium line pairs, with decreasing interspace ranging from 1 to 21 line pairs per centimetre. The highest spatial resolution providing indistinguishable line pairs was noted by the two readers independently.

– *Signal to Noise Ratio:*

To determine signal to noise ratio, image analysis software was used (Artiscan, Aquilab, France). The SNR was evaluated on axial images, with the CTP486 Image uniformity module, using the following formula (Eq. 2):

$$SNR = \sqrt{2}\frac{D_{Phantom}}{SD_{Phantom}}$$

Where $D_{Phantom}$ corresponds to the mean density of a ROI encompassing the entire uniformity module in transverse plane and $SD_{Phantom}$ corresponds to the mean standard deviation measured within the ROI. Two consecutive scan acquisitions of the Catphan phantom were performed to provide a mean SNR ratio.

Table 4 Mean density, noise, and signal to noise ratio (SNR) measured within the liver, spleen, lumbar muscle, abdominal subcutaneous fat, and air on all CT acquisition and reconstruction techniques. The highest SNR was observed on reduced-dose CT reconstructed using MBIR. *HU*, Hounsfield unit

Density measures	Standard-dose CT with FBP reconstruction	Reduced-dose CT with 50 % ASIR reconstruction	Reduced-dose CT with MBIR reconstruction	*p* (one-way ANOVA)
Liver density (HU) [Mean±SD]	97.2±12.6	121.8±18.4	121.1±11.5	$p<0.0001$
SNR	8.4	7.0	10.8	$p<0.0001$
Spleen density (HU) [Mean±SD]	100.5±13.2	130.0±18.5	129.3±11.6	$p<0.0001$
SNR	7.7	7.1	11.2	$p<0.0001$
Muscle density (HU) [Mean±SD]	55.4±12.8	63.0±17.2	63.7±11.3	$p=0.0017$
SNR	4.9	3.9	5.9	$p<0.0001$
Subcutaneous fat density (HU) [Mean±SD]	-103.5±13.5	-116.0±16.3	-118.2±11.5	$p=0.0001$
SNR	8.2	7.5	10.8	$p<0.0001$
Air density (HU) [Mean±SD]	-995.1±7.7	-972.0±10.2	-993.7±3.6	$p=0.35$
SNR	143.3	102.7	325.0	$p<0.0001$

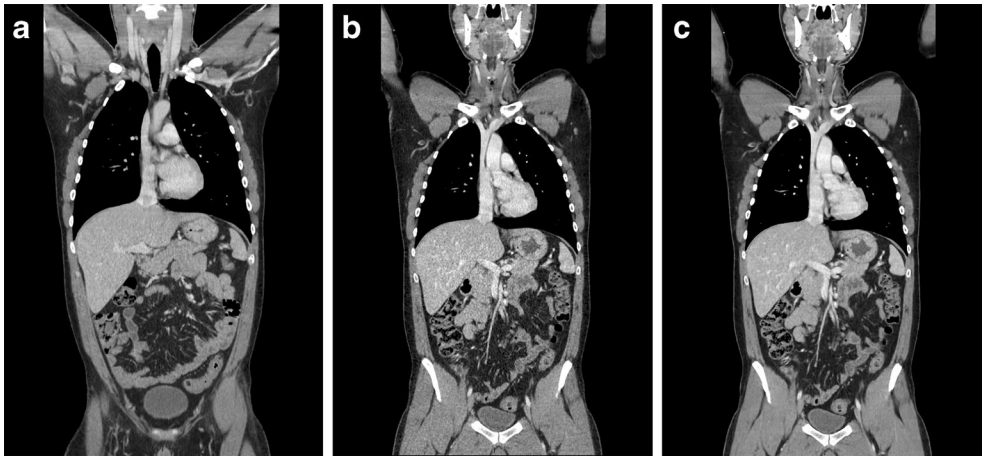

Fig. 1 31 year-old patient followed for stage III diffuse large B-cell lymphoma in complete remission on both standard-dose CT performed in November 2011 with FBP reconstruction (**a**), and on reduced-dose CT obtained 12 months later using 50 % ASIR (**b**) and MBIR reconstruction algorithm (**c**). The mean dose is significantly higher with the standard-dose protocol than with the reduced-dose protocol (respectively, CTDIvol = 11.14 mGy and CTDIvol = 3.62 mGy; respectively, DLP of 885 mGy.cm and of 301 mGy.cm)

Statistical analysis

The mean CTDIvol, DLP and helical length were compared for each patient on the standard-dose CT and the reduced-dose CT (two independent samples t-test). For each organ, and for each reconstruction of both standard-dose CT and reduced-dose CT, variations in both mean organ density, and signal to noise ratio were compared by one-way analysis of variance (ANOVA) followed by Bonferroni post-hoc test. For each CT acquisition and each reconstruction technique, low contrast detectability, spatial resolution, and signal to noise ratio of the Catphan 600 phantom were compared (Kruskall Wallis followed by Dunn post-hoc test). $p<0.05$ was considered to indicate a statistically significant difference. All statistical analyses were conducted using XL STAT®, 2013 version 5.09, for Windows (Microsoft, Inc).

Results

Patients study

Dosimetric analysis

The mean CTDIvol, DLP, and length of acquisition for the standard-dose CT and the reduced-dose CT are presented in Table 3. Both the CTDIvol and the DLP were significantly lower on the reduced-dose CT ($p<0.0001$) while the length of acquisition was higher on the reduced-dose CT ($p=0.018$).

Image analysis

The mean densities of all ROIs within the selected organs are shown in Table 4. Identical mean densities were found for air, whatever acquisition and reconstruction protocol (one-way ANOVA; $p=0.35$). The mean densities of liver, spleen,

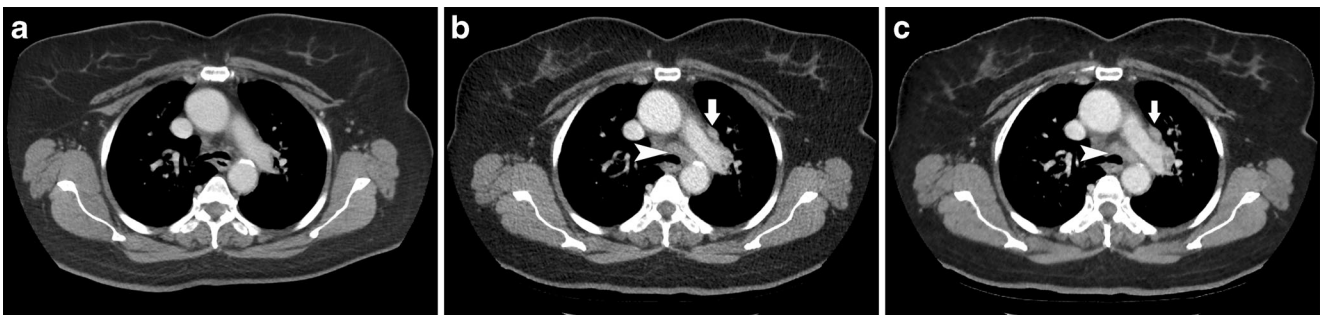

Fig. 2 71 year-old patient, followed up for stage IV diffuse large B-cell lymphoma in complete remission on standard-dose CT performed in December 2011 with FBP reconstructions (**a**). In October 2012, the reduced-dose CT suggested disease relapse with enlarged supra-diaphragmatic lymph nodes, which were well depicted both on 50 % ASIR- (*arrow* and *arrowhead*, **b**) and on MBIR-reconstructed (*arrow* and *arrowhead*, **c**) images. Disease relapse was confirmed by ^{18}F-FDG-PET-CT and biopsy. The CT dose was significantly lower on reduced-dose CT than on standard-dose CT (respectively, CTDIvol of 6.06 and 20.0 mGy)

muscle and fat varied among reconstructions (one-way ANOVA, $p<0.001$), with lowest densities found on standard-dose CT scan acquisition (Bonferroni post test p value <0.009), which are performed at higher kV. Examples of CT acquisition performed in identical patients using standard-dose CT or reduced-dose CT and with different reconstruction techniques are shown in Figs. 1 and 2.

The variations of noise and SNR according to the CT acquisition and reconstruction techniques are shown in Fig. 3. The mean noise and SNR of liver, spleen, muscle, and air varied among reconstructions (one-way ANOVA, $p<0.0001$). For each organ, the mean noise was lower with MBIR, and significantly lower for the spleen, air, and fat measurements (respectively, $p=0.04$, $p=0.027$, and $p=0.0001$ with Bonferroni post test). For each organ, the mean SNR was significantly higher on MBIR reconstructed images compared to ASIR or FBP for every organ (Bonferroni post test $p<0.02$).

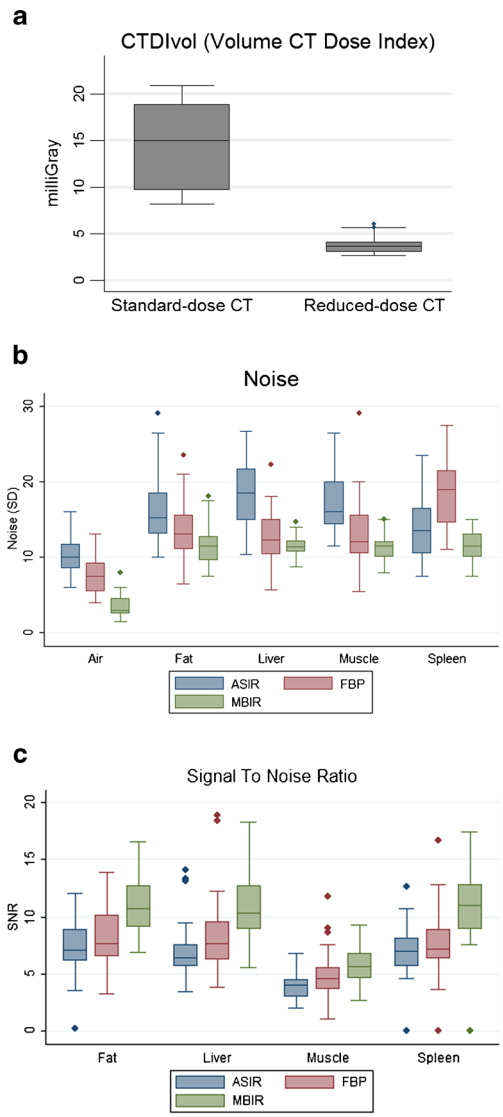

Fig. 3 Comparison of CTDIvol (**a**) noise (**b**) and signal to noise ratio (SNR) (**c**) in patients followed up with standard-dose CT or with reduced-dose CT and 50 % ASIR- or MBIR-reconstructed images. The mean dose is significantly reduced on reduced-dose CT, together with increased noise on 50 % ASIR-reconstructed images. On reduced-dose CT MBIR-reconstructed images, the noise is significantly reduced with increased SNR

Phantom study

The comparative analysis of phantom experiments is provided in Table 5. Neither low contrast detectability measurements nor spatial resolution varied significantly between the different reconstructions techniques. Every acquisition and reconstruction technique allowed the detection of up to seven or eight lines per centimetre. The SNR measurements were significantly different (Kruskall Wallis, $p=0.003$) between all acquisitions and reconstruction techniques with highest values observed with MBIR-reconstructed images obtained with the reduced-dose CT (mean SNR of 138±0.7) as opposed to 50 % ASIR reconstructed images obtained with the reduced-dose CT (mean SNR of 77±0.4; $p=0.001$) or FBP-reconstructed images obtained with the standard-dose CT (mean SNR of 85±1.0; $p=0.11$).

Discussion

Results of this study, focusing on follow-up body CT image acquisitions for lymphoma patients show that MBIR-reconstruction leads to reduced X-ray exposure with maintained objective image quality. Hence, mean CTDIvol values of 4.06 mGy can be reached in adult patients, results similar to recent reports in paediatric populations, or in various clinical applications [30, 32–38]. In addition, MBIR outperforms ASIR in terms of image quality, when using stringent acquisition parameters enabling very low-dose CT examinations.

The role of CECT for early response assessment has been recently questioned, as 18F-FDG-PET now plays a key role for metabolic assessment of tumour response in aggressive lymphoma [39]. However, CECT still plays a central role in lymphoma patient management: in close to 10 % of patients, CECT enables the detection of conditions un-related to lymphoma, such as pulmonary embolism, infections, or incidental findings [16]. Furthermore, CECT still remains today the cornerstone for the follow-up of many lymphoma patients, as still recommended by international work-groups [13–15] and international experts [17]. According to literature, X-ray exposition is a major inconvenient in lymphoma CT-surveillance, optimizing CECT acquisition and reducing dose is thus of utmost importance. In addition, dose reduction techniques could be applied to hybrid PET-CT modality or to simultaneous diagnosis CECT and PET-CT acquisition when required, performed at the lowest dose [16].

Table 5 Image quality parameters obtained on Catphan 600 phantom for all CT acquisition and reconstruction techniques. The number of targets at different low contrast detectability and the spatial resolution were similar with the different techniques used. The mean SNR was significantly higher on reduced-dose CT acquisitions reconstructed using MBIR.

Image quality parameters measured on Catphan 600 phantom	Standard-dose CT with FBP reconstruction	Reduced-dose CT with 50 % ASIRreconstruction	Reduced-dose CT with MBIR Reconstruction	*p* (KruskalWallis)
Number of targets [Mean±SD] at different low contrast detectability levels (%)	1 %: 5.6±0.7 0.5 %: 2.8±1.1 0.3 %: 0	1 %: 5.6±0.7 0.5 %: 2±0 0.3 %: 0	1 %: 5±1 0.5 %: 2.8±0.7 0.3 %: 0	1 %: p=0.47 0.5 %: p=0.24 0.3 %: p=N.A.
Spatial resolution (line Pairs) [Mean±SD]	7±0	7±0	7.4±0.4	p=0.11
SNR [Mean±SD]	85±1.0	77±0.4	138±0.7	p=0.003

The SNR observed on the reduced-dose CT was significantly improved using MBIR reconstruction algorithms when compared to 50 % ASIR. Interestingly, the level of noise within the images was similar between FBP reconstructed images using standard-dose CT acquisition parameters and MBIR-reconstructed images acquired with a reduced-dose CT that is four times less than the standard. The mean density values were, however, different between standard-dose CTs and reduced-dose CT acquisition. This difference is directly related to the different tube voltage used in both protocols – namely 120 kV for standard-dose CT imaging protocol and 100 kV for reduced-dose CT protocol. Such difference was previously observed [40–42]. In addition, a lower tube voltage favours the attenuation of contrast material, owing to greater photoelectric effect and decreased Compton scattering. It is noteworthy that the densities measured in the study concerned contrast-enhanced acquisitions, which accounts for the relatively high mean densities of liver, spleen, and muscle recorded in this study.

To our knowledge, few studies have compared ASIR and MBIR using objective criteria [33]. This is especially important as the use of subjective criteria is hampered by the absence of a truly blinded evaluation: MBIR, ASIR, and FBP reconstructed images all have different appearances that are unique and recognizable. Also, the use of a phantom allowed the comparison between both low contrast resolution detectability and spatial resolution. Moreover, the SNR was significantly improved with MBIR reconstructions, while the average dose was decreased, results in accordance with previous publications [28]. MBIR also significantly reduces the noise within the image, which was observed in this patient study.

Volders et al. [30] have suggested that a lower threshold value for CTDIvol of 5.18 mGy could be targeted for clinical practice when dealing with liver metastases. Interestingly, the CTDIvol values obtained on reduced-dose CT in our study are even lower. The clinical rationale in lymphoma patients is different from that of patients with liver metastases: the challenge for contrast enhanced CT (CECT) is to provide optimal staging at baseline and detection of relapse on follow-up.

One limitation of the study is that all but one patient was in complete remission. However, our aim was first to test the objective performance of MBIR in reduced-dose CT performed on phantoms and in patients at low risk of tumour recurrence. Future studies should be carried out in order to prospectively evaluate MBIR, together with PET-CT for baseline staging and response assessment, in order to detect both nodal and organ involvement by lymphoma. Furthermore, radiation dose and objective image quality are independent of lymphoma treatment response. This study also suggests that MBIR-reconstructed images obtained with reduced-dose acquisitions and FBP-reconstructed images obtained with standard-dose acquisitions share the same contrast detectability on phantom. Reduced-dose CT imaging parameters were specifically selected to significantly impact dose reduction. Moreover, CT doses were compared with CT examinations performed without ASIR capacity. However, a 4.06 mGy CTDIvol provides noisy raw images where ASIR reconstructions appear insufficient to restore sufficient SNR.

Overall, the use of reduced-dose CT together with MBIR reconstruction can significantly decrease radiation dose delivered to patients followed for lymphoma, while keeping an image quality similar to that obtained on standard-dose CT. Prospective trials could further evaluate the role of such reduced-dose CECT together with ^{18}F-FDG PET CT for lymphoma patients management.

Acknowledgments The scientific guarantor of this publication is Professor Alain Luciani MD PHD. Philippe Richard is an employee from GE Healthcare France. All non industrial authors belong to the CHU Henri Mondor institution and were always in control of data processing. The authors state that this work has not received any funding. No complex statistical methods were necessary for this paper. Institutional review board approval was obtained (IRB 00003835). Written informed consent was waived by the Institutional Review Board. Methodology: retrospective, observational, performed at one institution.

References

1. Brenner DJ, Hall EJ (2007) Computed tomography–an increasing source of radiation exposure. N Engl J Med 357:2277–2284
2. Mettler FA Jr, Thomadsen BR, Bhargavan M et al (2008) Medical radiation exposure in the U.S. in 2006: preliminary results. Health Phys 95:502–507
3. Mettler FA, Bhargavan M, Faulkner K et al (2009) Radiologic and nuclear medicine studies in the United States and worldwide: frequency, radiation dose, and comparison with other radiation sources—1950–20071. Radiology 253:520–531
4. Bernier MO, Rehel JL, Brisse HJ et al (2012) Radiation exposure from CT in early childhood: a French large-scale multicentre study. Br J Radiol 85:53–60
5. Hall EJ, Brenner DJ (2008) Cancer risks from diagnostic radiology. Br J Radiol 81:362–378
6. Mathews JD, Forsythe AV, Brady Z et al (2013) Cancer risk in 680 000 people exposed to computed tomography scans in childhood or adolescence: data linkage study of 11 million Australians. BMJ 346
7. Pearce MS, Salotti JA, Little MP et al (2012) Radiation exposure from CT scans in childhood and subsequent risk of leukaemia and brain tumours: a retrospective cohort study. Lancet 380:499–505
8. Brenner DJ, Hall EJ (2012) Cancer risks from CT scans: now we have data, what next? Radiology 265:330–331
9. Gardavaud F, Luciani A, Rahmouni A (2012) CT scans in childhood and risk of leukaemia and brain tumours. Lancet 380:1735, author reply 1736-1737
10. Tubiana M, Feinendegen LE, Yang C, Kaminski JM (2009) The linear no-threshold relationship is inconsistent with radiation biologic and experimental data1. Radiology 251:13–22
11. Journy N, Rehel JL, Ducou Le Pointe H et al (2014) Are the studies on cancer risk from CT scans biased by indication? Elements of answer from a large-scale cohort study in France. Br J Cancer. doi:10.1038/bjc.2014.526
12. Recher C, Coiffier B, Haioun C et al (2011) Intensified chemotherapy with ACVBP plus rituximab versus standard CHOP plus rituximab for the treatment of diffuse large B-cell lymphoma (LNH03-2B): an open-label randomised phase 3 trial. Lancet 378:1858–1867
13. Dreyling M, Thieblemont C, Gallamini A et al (2013) ESMO Consensus conferences: guidelines on malignant lymphoma. part 2: marginal zone lymphoma, mantle cell lymphoma, peripheral T-cell lymphoma. Ann Oncol. doi:10.1093/annonc/mds643
14. Tilly H, Vitolo U, Walewski J et al (2012) Diffuse large B-cell lymphoma (DLBCL): ESMO Clinical Practice Guidelines for diagnosis, treatment and follow-up. Ann Oncol 23:vii78–vii82
15. Zelenetz AD, Gordon LI, Wierda WG et al (2014) Non-Hodgkin's lymphomas, version 4.2014. J Natl Compr Cancer Netw 12:1282–1303
16. Chalaye J, Luciani A, Enache C et al (2014) Clinical impact of contrast-enhanced computed tomography combined with low-dose F-fluorodeoxyglucose positron emission tomography/computed tomography on routine lymphoma patient management. Leuk Lymphoma. doi:10.3109/10428194.2014.900761
17. Cheson BD, Fisher RI, Barrington SF et al (2014) Recommendations for initial evaluation, staging, and response assessment of Hodgkin and non-Hodgkin lymphoma: the Lugano classification. J Clin Oncol. doi:10.1200/jco.2013.54.8800
18. Fleischmann D, Boas FE (2011) Computed tomography–old ideas and new technology. Eur Radiol 21:510–517
19. Kaza RK, Platt JF, Goodsitt MM et al (2014) Emerging techniques for dose optimization in abdominal CT. Radiographics 34:4–17
20. Beister M, Kolditz D, Kalender WA (2012) Iterative reconstruction methods in X-ray CT. Phys Med 28:94–108
21. Hara AK, Paden RG, Silva AC, Kujak JL, Lawder HJ, Pavlicek W (2009) Iterative reconstruction technique for reducing body radiation dose at CT: feasibility study. AJR Am J Roentgenol 193:764–771
22. Leipsic J, Labounty TM, Heilbron B et al (2010) Adaptive statistical iterative reconstruction: assessment of image noise and image quality in coronary CT angiography. AJR Am J Roentgenol 195:649–654
23. Marin D, Nelson RC, Schindera ST et al (2010) Low-tube-voltage, high-tube-current multidetector abdominal CT: improved image quality and decreased radiation dose with adaptive statistical iterative reconstruction algorithm—initial clinical experience1. Radiology 254:145–153
24. Silva AC, Lawder HJ, Hara A, Kujak J, Pavlicek W (2010) Innovations in CT dose reduction strategy: application of the adaptive statistical iterative reconstruction algorithm. AJR Am J Roentgenol 194:191–199
25. Singh S, Kalra MK, Hsieh J et al (2010) Abdominal CT: comparison of adaptive statistical iterative and filtered back projection reconstruction techniques. Radiology 257:373–383
26. Thibault JB, Sauer KD, Bouman CA, Hsieh J (2007) A three-dimensional statistical approach to improved image quality for multislice helical CT. Med Phys 34:4526–4544
27. Hsieh J, Nett B, Yu Z, Sauer K, Thibault J-B, Bouman C (2013) Recent advances in CT image reconstruction. Curr Radiol Rep 1:39–51
28. Smith EA, Dillman JR, Goodsitt MM, Christodoulou EG, Keshavarzi N, Strouse PJ (2013) Model-based iterative reconstruction: effect on patient radiation dose and image quality in pediatric body CT. Radiology. doi:10.1148/radiol.13130362
29. Choo JY, Goo JM, Lee CH, Park CM, Park SJ, Shim MS (2013) Quantitative analysis of emphysema and airway measurements according to iterative reconstruction algorithms: comparison of filtered back projection, adaptive statistical iterative reconstruction and model-based iterative reconstruction. Eur Radiol. doi:10.1007/s00330-013-3078-5
30. Volders D, Bols A, Haspeslagh M, Coenegrachts K (2013) Model-based iterative reconstruction and adaptive statistical iterative reconstruction techniques in abdominal CT: comparison of image quality in the detection of colorectal liver metastases. Radiology. doi:10.1148/radiol.13130002
31. Cheson BD, Pfistner B, Juweid ME et al (2007) Revised response criteria for malignant lymphoma. J Clin Oncol 25:579–586
32. Katsura M, Matsuda I, Akahane M et al (2012) Model-based iterative reconstruction technique for radiation dose reduction in chest CT: comparison with the adaptive statistical iterative reconstruction technique. Eur Radiol 22:1613–1623
33. Deak Z, Grimm JM, Treitl M et al (2013) Filtered back projection, adaptive statistical iterative reconstruction, and a model-based iterative reconstruction in abdominal CT: an experimental clinical study. Radiology 266:197–206
34. Gonzalez-Guindalini FD, Botelho MP, Tore HG, Ahn RW, Gordon LI, Yaghmai V (2013) MDCT of chest, abdomen, and pelvis using attenuation-based automated tube voltage selection in combination with iterative reconstruction: an intrapatient study of radiation dose and image quality. AJR Am J Roentgenol 201:1075–1082
35. Ichikawa Y, Kitagawa K, Nagasawa N, Murashima S, Sakuma H (2013) CT of the chest with model-based, fully iterative reconstruction: comparison with adaptive statistical iterative reconstruction. BMC Med Imaging 13:27
36. Nishida J, Kitagawa K, Nagata M, Yamazaki A, Nagasawa N, Sakuma H (2013) Model-based iterative reconstruction for multi–detector row CT assessment of the Adamkiewicz artery. Radiology. doi:10.1148/radiol.13122019
37. Shuman WP, Green DE, Busey JM et al (2013) Model-based iterative reconstruction versus adaptive statistical iterative reconstruction and filtered back projection in liver 64-MDCT: focal lesion detection, lesion conspicuity, and image noise. AJR Am J Roentgenol 200:1071–1076
38. Vardhanabhuti V, Ilyas S, Gutteridge C, Freeman SJ, Roobottom CA (2013) Comparison of image quality between filtered back-projection and the adaptive statistical and novel model-based iterative reconstruction techniques in abdominal CT for renal calculi. Insights Imaging 4:661–669

39. Haioun C, Itti E, Rahmouni A et al (2005) [18F]fluoro-2-deoxy-D-glucose positron emission tomography (FDG-PET) in aggressive lymphoma: an early prognostic tool for predicting patient outcome. Blood 106:1376–1381
40. Coppenrath E, Meindl T, Herzog P et al (2006) Dose reduction in multidetector CT of the urinary tract. Studies in a phantom model. Eur Radiol 16:1982–1989
41. Bjorkdahl P, Nyman U (2010) Using 100- instead of 120-kVp computed tomography to diagnose pulmonary embolism almost halves the radiation dose with preserved diagnostic quality. Acta Radiol 51: 260–270
42. Avrin DE, Macovski A, Zatz LE (1978) Clinical application of Compton and photo-electric reconstruction in computed tomography: preliminary results. Investig Radiol 13:217–222